ELSEVIER

Synthesis and characterization of porous β-tricalcium phosphate blocks

M. Bohner[a],*, G.H. van Lenthe[b], S. Grünenfelder[a], W. Hirsiger[a], R. Evison[b], R. Müller[b]

[a]*Dr H.C. Robert Mathys Foundation, Bischmattstrasse 12, CH-2544 Bettlach, Switzerland*
[b]*Institute for Biomedical Engineering, Swiss Federal Institute of Technology (ETH) and University of Zürich,
Moussonstrasse 18, CH-8044 Zürich, Switzerland*

Abstract

Porous β-tricalcium phosphate (β-TCP) blocks with four different macropore sizes (pore larger than $50\,\mu m$) were synthesized using "calcium phosphate emulsions", and characterized by optical, geometrical, gravimetric, and radiological methods. The reproducibility of the synthesis method was excellent. Moreover, the macropore size could be easily controlled without modifying the microporosity (pore smaller than $50\,\mu m$) or the total porosity (microporosity + macroporosity). Based on the initial composition of the blocks and their final apparent density, the microporosity, macroporosity, and the total block porosity were calculated to be close to 21%, 54%, and 75%, respectively. These values were confirmed by microcomputed tomography (μCT). The mean macropore diameters were close to 150, 260, 510 and $1220\,\mu m$, as measured optically. Consistently lower values (25% lower) were obtained by μCT, but the linear correlation between μCT and optical method was high ($r^2 > 0.97$). The macropore size distribution calculated from μCT scans appears to be narrow and normally distributed. The very good correlation between the results of the various methods and the possibility to determine the pore size distribution suggest that μCT is an ideal tool to non-destructively characterize macroporous calcium phosphate bone substitutes.

1. Introduction

Since calcium phosphate materials started being used as bone substitute materials, researchers have been interested in determining the optimum pore structure [1–6]. This task is not easy for three reasons: (i) it is difficult to synthetize ceramics with perfectly controlled geometries, (ii) most in vivo studies have only considered few pore structures (e.g. 1 or 2) at few implantation times (e.g. 1 or 2), and (iii) the results might depend on the rate of resorption of the investigated bone substitute (e.g. different optimum for β-tricalcium phosphate (β-TCP) and hydroxyapatite).

Nevertheless, most studies suggested that (i) a pore diameter in the range of $100–1000\,\mu m$ is adequate [1–6], (ii) pores should be interconnected, and (iii) the size of the interconnections should be larger than about $50\,\mu m$ [4]. The recent developments in tissue engineering have triggered previous efforts even more. However, the requirements of tissue engineering where cells are grown in a "test tube" without blood supply might be different from those of bone substitutes in vivo. So, the requirements for cell seeding, bone ingrowth, and bone substitute resorption should be considered separately.

Keeping that in mind, Bohner and Baumgart [7] used a theoretical approach to determine an adequate porous structure to minimize the resorption time. These authors found out that a pore diameter in the range of $200–800\,\mu m$ is optimal, but that this optimum depends

*Corresponding author. Tel.: +41 32 6441413; fax: +41 32 6441176.
E-mail address: marc.bohner@rms-foundation.ch (M. Bohner).

on the size of the bone substitute: larger pieces require larger pores (keeping the total porosity constant). To test the adequacy of the model, a new in vivo study was performed in which resorbable β-TCP blocks with four different pore sizes were implanted in sheep metaphyseal defects for 6, 12, and 24 weeks. The goal was to implant blocks that only differed in one feature, i.e. pore size, in order to assess the effect of the latter feature (pore size) on resorption. Considering the promising results obtained with the so-called calcium phosphate emulsion method [8], all β-TCP blocks were synthesized with the latter method. However, before implantation, adequate morphological characterization of these blocks was required. Therefore, the two main goals of the present study were (i) to present the synthesis and characterization methods of these four types of β-TCP blocks and (ii) to determine the suitability of micro-computed tomography (μCT) to non-destructively characterize porous ceramic blocks.

2. Materials and methods

The blocks were produced with the so-called "calcium phosphate emulsions" method [8], which is used to produce a commercially available bone substitute (chronOS^{TM}, Synthes Biomaterials, Bettlach, Switzerland). Briefly, to produce one batch, 80 g α-tricalcium phosphate (α-TCP; produced in-house) and 20 g TCP (Merck, Germany) were added to 100 g viscous paraffin oil (Merck, Dietikon, Switzerland) and 67 mL of a solution containing polyethoxylated castor oil (PECO; product name "Cremophor EL", BASF, Wädenswil, Switzerland), 1% 5.1 kDa poly(acrylic acid) (Fluka, Buchs, Switzerland), and 0.2 M Na_2HPO_4 solution. These components were stirred at 2000 RPM with a stirring bar for 45 s. The resulting paste consisted in a metastable mixture of a calcium phosphate cement paste in which small oil droplets were dispersed. The size of the droplets depended on the concentration of emulsifier (PECO). Four concentrations of PECO were used: 0.017 (batch 4), 0.14 (batch 3), 0.30 (batch 2), and 0.57 g/L (batch 1). After 90 s, the resulting paste was poured into eight moulds, incubated for 24 h until complete hardening occurred, cleaned with petroleum ether, dried and finally sintered at 1250 °C to obtain phase-pure β-TCP (as observed by X-ray diffraction). Two batches were produced per PECO concentration (e.g. batch 4.1 and 4.2 with 0.017 g/L emulsifier concentration). The samples were then machined to obtain cylinders 8 mm in diameter and 13 mm in length. Typically, 1–3 cylinders were obtained per sample, depending on the sample size. Eight samples were obtained per batch resulting in a total of 15–20 cylinders per batch. From these 15–20 cylinders, nine specimens were (randomly) retrieved for each batch and their morphology was analyzed more carefully. The results of these characterizations are described in detail in this document. Five additional samples were tested mechanically to determine their compressive strength.

The pore structure of the samples was characterized by calculating their macroporosity (assuming that the initial volume fraction of oil corresponds to the final macroporosity) by measuring their apparent density (the total porosity can then be estimated knowing the theoretical density of β-TCP ≈ 3.1 g/cm^3), and by determining their average macropore size based on optical photos of the block surface (Leica MZ12 microscope, JVC KY-F70 digital camera, Image Access software). For that purpose, the average diameter of fifteen macropores of the block surface was determined and an average macropore diameter, D^e, was calculated. The final macropore diameter, D, was calculated from D^e via the following equation (assuming that all the macropores are round): $D = \sqrt{(3/2)} D^e$. In addition to these methods, the two ends of the samples left after machining were coated with carbon and observed by scanning electron microscopy (SEM; Cambridge S360) to determine the appearance of the microporosity and possible structural changes between the bottom and the top of each sample.

For non-destructive three-dimensional (3D) characterization of the samples, all blocks were scanned and analyzed by μCT, also referred to as desktop μCT [9], using a commercial imaging device (μCT 40, Scanco Medical AG, Bassersdorf, Switzerland). A microfocus X-ray tube with a focal spot of 7 μm was used as a source. Measurements were stored in 3D image arrays with an isotropic voxel size of 30 μm. Besides assessing visually the block images, morphometric parameters were determined from the μCT datasets using direct 3D morphometry [10]. In particular, the macropore size distribution was determined using the distance transformation method [11]. In this method, each macropore is filled with a non-redundant set of maximal spheres. Mean pore size can then be calculated as the average diameter of all spheres making up the pore. To exclude errors resulting from the cutting of the samples, a thin layer at the boundary of the sample was automatically excluded from the 3D reconstructions. Based on the macropore size distribution, a mean and median macropore diameters were calculated (volume weighed).

3. Results

3.1. General appearance

The morphology of the blocks can be seen on Figs. 1–3. To discuss these morphologies, it is important to define two types of pores: micro- and macropores. These pores are distinguished by their size: micropores
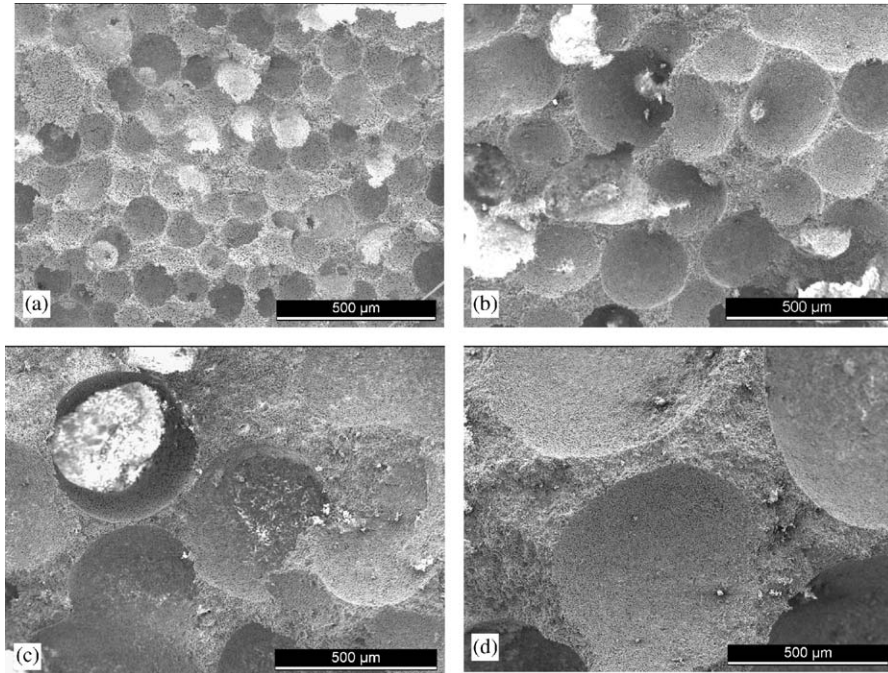
Fig. 1. Representative SEM photos of the four different macropores sizes (increasing size from (a) to (d)). The white bar corresponds to 0.5 mm.
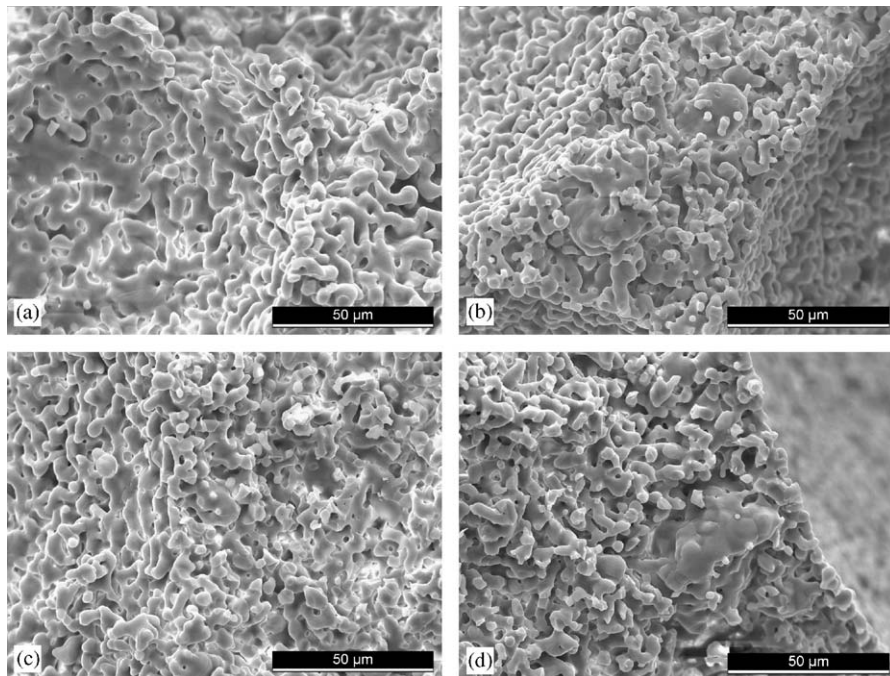

Fig. 2. SEM photo of the four different macropores sizes (increasing size from (a) to (d)). The white bar corresponds to 50 μm.

have a diameter typically close to 1–20 μm, whereas macropores have a diameter > 100 μm. The threshold is placed at a size of 50 μm.

A look at Figs 1–3 show that the four different emulsifier concentrations led to four different macropore sizes (Figs 1 and 3), but did not modify the micropore size (Fig 2). The macropores were rather spherical and partly interconnected, independent of their size. Micropores were elongated and apparently fully interconnected (Fig 2).

The corners of the block with the smallest pore size (Fig 3, top left) appeared to be fully dense on the μCT
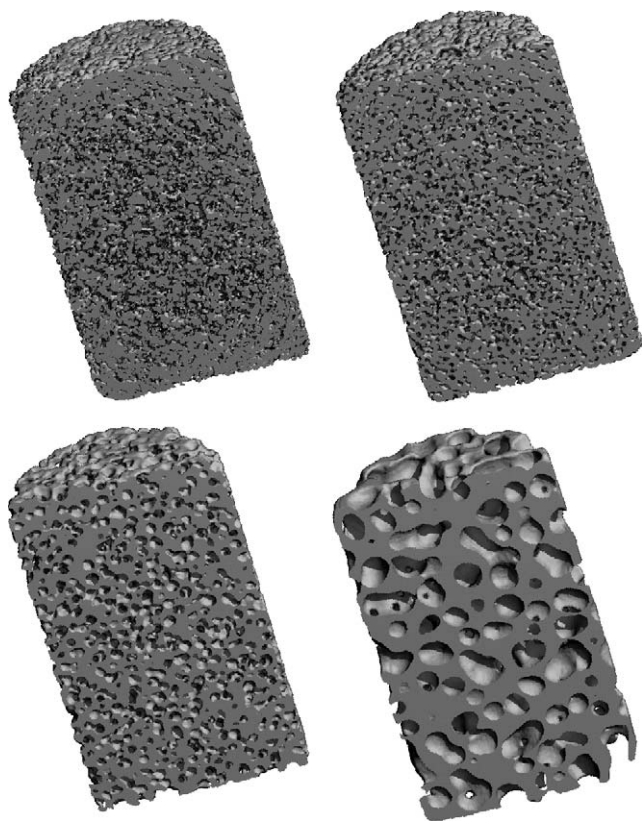
Fig. 3. Typical μCT scans of the four different blocks.

scan even though optically no difference could be detected. This effect was less important with a smaller pixel size (data not shown).

3.2. Quantitative results

The total block porosity determined from apparent density measurements was rather constant from batch to batch, as values ranged from 73.5% to 76.6% (Table 1). However, these small differences were in all but one case highly significant ($p < 0.005$). In fact, the only difference that was less significant (i.e. $p < 0.036$) was the difference between the emulsifier concentrations 0.570 and 0.300 (difference between batches 1.1, 1.2 and 2.1, 2.2, respectively). In all these cases, the trend was an increase of porosity with a decrease of macropore size. The porosities extracted from μCT data (μCT porosity) were all close to 53–54% except for batch 2 (64.4).

The mean macropore sizes determined by the optical method were close to 150, 260, 510, and 1220 μm (Table 1). Little variation was found between batches and samples within batches, as expressed by the small standard deviations (Table 1). Moreover, top and bottom part of samples did not have significantly different geometries. Similar but lower diameters were obtained with μCT: 140, 180, 360, and 900 μm (Table 1).

As seen for optical measurements, little variation was found from sample to sample within a batch.

The macropore size distributions were narrow and could be well described by a normal distribution (Fig. 4, Table 2). These two features were expressed by a relatively small coefficient of variation of the distribution (ratio of standard deviation and mean given in percent), and a high coefficient of determination r^2 from the regression of mean and standard deviation for all samples (Table 2). Moreover, the mean and the median of the pore size were almost identical, suggesting a symetrical pore size distribution. Little variation was seen between batches, particularly at large macropore sizes.

The macropore interconnectivity was defined as the number of interconnections per pore. This factor increased from 0.4 to 0.5 (interconnections per pore) at high emulsifier concentration, i.e. from 0.57 g/L, to 2.0–2.1 g/L at intermediate concentration, i.e. 0.140 g/L, before decreasing to 1.2 at low concentration, i.e. 0.017 g/L (Table 1).

When the weight of the cylinders was plotted as a function of their X-ray density, a linear regression was obtained, demonstrating a good correlation between apparent density (and hence total porosity) and μCT data ($r^2 > 0.96$). Similarly, a high correlation ($r^2 > 0.97$) was found between the macropore diameter determined by μCT and the value determined by optical methods.

4. Discussion

The goal of the present study was twofold: (i) present the synthesis of β-TCP blocks with various pore sizes using the so-called calcium phosphate emulsion method [8], and (ii) characterize their morphology via gravimetric, optical and radiological methods. In the present discussion, both topics are discussed separately in a successive manner.

4.1. Synthesis method

The new synthesis method presented in this study which is based on mixtures of calcium phosphate cement paste and paraffin oil proved to be very reproducible, as evidenced by the small deviations of the compressive strength, the macropore size and macropore volume within a batch and between batches (Table 1).

The synthesis method enabled to obtain spherical macropores where size could be easily modified by a change of emulsifier concentration. The spherical shape was the result of the presence in the cement paste of oil droplets stabilized by small amounts of emulsifier.

A change of emulsifier concentration changed the macropore size (Fig. 1) but apparently not the microporosity (Fig. 2). This is expected since the oil droplets

Table 1
Properties of the various batches

Batch no.	1.1	1.2	2.1	2.2	3.1	3.2	4.1	4.2
Emulsifier (g/L)	0.570	0.570	0.300	0.300	0.140	0.140	0.017	0.017
Porosity (%)	75.1	73.5	75.7	74.1	76.1	75.4	76.6	75.9
SD[a] (vol%)	0.4	0.6	1.1	0.5	0.4	0.3	0.6	0.4
Macropore diameter	149	157	276	253	505	509	1191	1251
SD[a] (μm)	14	7	18	16	24	39	114	92
(Macro)Porosity[b]	64.4	54.1	57.1	52.6	54.5	53.1	54.0	53.5
SD[a] (vol%)	2.4	4.5	3.3	1.3	1.0	0.4	0.7	0.9
Mean macropore diameter[b]	156	132	189	173	362	357	916	889
SD[a] (μm)	8	7	6	5	13	10	20	24
Median macropore diameter[b]	150	127	180	170	360	360	921	890
SD[a] (μm)	0	13	0	15	0	0	14	21
Connectivity[b,c]	0.38	0.50	1.33	1.24	2.12	2.03	1.25	1.20
SD[a] (μm)	0.05	0.05	0.09	0.08	0.07	0.11	0.11	0.11

The theoretical density of β-TCP (3.1 g/cm^3) was used to calculate the porosity from the apparent block density. The macroporosity calculated from the block composition is 53.6%. The difference of porosity between batch 1 and 2 was not as significant ($p < 0.036$) as the difference between all other batches ($p < 0.005$; e.g. between batch 1 and 3 or between batch 2 and 4, etc…).
[a]SD = standard deviation.
[b]Determined using μCT.
[c]Ratio between the number of interconnections per volume and the number of pore per volume.

Table 2
Fitting parameters of the normal distribution $\left(y = (\alpha/\sqrt{2\pi}\sigma)e^{-(x-\mu)^2/(2\sigma^2)} \right)$ adjusted on the pore size distribution data (Fig. 4)

Batch no.	1.1	1.2	2.1	2.2	3.1	3.2	4.1	4.2
Proportionality constant, α	2.97	2.89	2.93	2.93	2.83	2.84	2.87	2.81
Mean, μ (μm)	147	125	180	166	358	355	920	890
Standard deviation, σ (μm)	46	35	33	31	44	45	146	141
Coefficient of determination, r^2	0.987	0.992	0.994	0.989	0.994	0.994	0.977	0.983
Coefficient of variation (%)	31.4	28.4	18.1	18.4	12.3	12.6	15.8	15.9

which are dispersed within the calcium phosphate cement paste to form macropores are far too large to interact with the cement microstructure.

Interestingly, the macropore size distribution became (relatively) narrower with a decrease of the emulsifier concentration (except for the smaller concentration; Fig. 4). This was expressed by a decrease in the coefficient of variation with increasing mean macropore size (Table 2). The reason for this effect is not clear, but might also be partly related to the relatively low resolution chosen for the μCT scanning (30 μm in this study) compared to the mean pore size.

The macropores were rather spherical (Figs. 1 and 3), but were not homogeneously dispersed within the block. As a result macropore interconnections were observed (Figs. 1 and 3). However, the structures were not fully interconnected, as the number of interconnections per pore was always lower than 3 (Table 1). This is probably due to the fact that the macroporosity (54%) was lower

than the minimum macroporosity (63%) required to obtain a fully interconnected structure (when macropores are spherical, monosized and randomly distributed [12]). Interestingly, the interconnectivity varied quite markedly with a change of macropore size (from 0.4 to 2.1 interconnections per pore) even though such large differences could not be expected from optical and SEM photos (Fig. 1). The low interconnectivity value obtained at the smallest macropore size could be an artefact of relatively low μCT resolution compared to the mean pore size (as previously discussed). The presence of interconnections is expected to have a positive effect on the in vivo response because it should allow a fast bone ingrowth. The presence of interconnections is related to the instability of the paste during setting: cement hardening destabilizes the emulsion, hence leading to the agglomeration and fusion of oil droplets.

One assumption that had been made about the synthesis method was that the macropore distribution
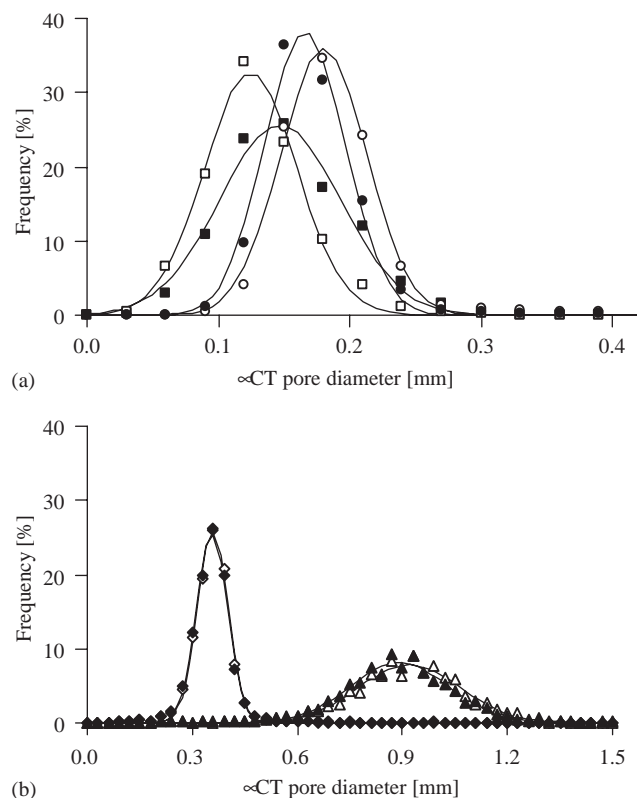
Fig. 4. Macropore size distribution derived from μCT scans. Symbols of chart (a): (■) batch 1.1; (□) batch 1.2; (●) batch 2.1; (○) batch 2.2. Symbols of chart (b): (◆) batch 3.1; (◇) batch 3.2; (▲) Batch 4.1; (△) batch 4.2. Normal distributions were fitted on the data. The regression parameters and the regression coefficient are given in Table 2.

was not a function of emulsifier concentration. In other words, a homothetic enlargement of the structure of e.g. batch 1.1 was expected to lead to e.g. batch 3.1, the enlargement ratio being the macropore size ratio. If this assumption was correct, the coefficient of variation of the normal distribution fitted on the data should not vary as a function of macropore size. A slightly different result was found (Table 2) as this ratio tended to decrease with an increase of macropore size. However, this effect was moderate and might be due to the difficulties to distinguish macropores and macropore interconnections, particularly at small macropore sizes where the pixel size (30 μm) is relatively large compared to the macropore size.

To summarize, the synthesis method leads to reproducible and controlled structures. Indeed, the macropore size can be modified very easily with the emulsifier concentration without modifying the total pore volume and the microporosity. The pore size distribution appears to be narrow and distributed normally. Finally, the method leads to a certain number of interconnections, but the structure does not appear to be fully interconnected.

4.2. Microcomputed tomography

As previously mentioned, the present study is part of a larger study in which a resorption model [7] has to be tested in vivo. The blocks characterized in this study are therefore meant to be implanted in a sheep model. Since it is of importance to localize the resorption areas of the ceramic and the position of new bone, it was decided to characterize each implanted block before implantation and after explantation by means of μCT. As this method has not been used very often to characterize porous ceramic blocks, it is of great interest to assess its adequacy.

The present results indicate that μCT is an excellent method to determine the micro-, macro-, and total porosity of the blocks. The porosity determined by μCT is in most cases very close to the macroporosity calculated from the paste composition (53.6%, Table 1). Therefore, these measurements must correspond to the macroporosity of the blocks. The high linear correlation observed between X-ray density and physical mass suggests that the total weight of a sample can be determined from the X-ray density and a calibration curve (regression line of the data). Knowing the size of the block, the apparent density and hence the total porosity can be determined. Finally, microporosity can be deducted from the difference between total porosity and macroporosity. Microporosity could not be detected directly from μCT scans because the size of micropores is smaller than the chosen μCT resolution (30 μm in the present study).

The discrepancy between the macropore size measured optically and via μCT is likely to be due to the algorithm used to calculate the size and to the surface roughness. In the optical method, the macropores are assumed to be spherical which is not fully the case here. Additionally, all macropores are assumed to be visible on the block surface, which was not the case because the block surface was not polished (only machined) prior to the measurements. Therefore, small intersected macropores were confounded with the surface roughness, and as a result, the mean macropore size tended to be overestimated. In contrast to this, in the μCT method, the macropores were not assumed to be spherical but were fitted with a set of maximal spheres yielding in an average pore size that will be determined as the weighed average of all spheres. This also means that any deviation from the perfect sphere in the pore shape will reduce the average pore size because this will introduce smaller spheres that fill this extra spaces. Moreover, macropores are often interconnected and therefore again smaller spheres will be fitted in these connections reducing again the average pore size. These two effects led to an underestimation of the macropore size using a model-independent direct 3D approach as compared to the optical method.

At the smallest pore size, dense corners were observed on the µCT scans (Fig. 3). Moreover, the macroporosity of batch 2 (64%) determined by µCT was much higher than the value measured for other batches ($\approx 54\%$; Table 1). Furthermore, the macropore size determined by µCT for the smallest pore diameter (140 µm) was almost the same as the value measured for the second smallest pore diameter (180 µm), despite the fact that a much larger difference was observed optically (Fig. 1). These results suggest that the limits of the µCT method were reached. This is understandable as the chosen pixel size (30 µm) was relatively large. Better results were obtained with a higher resolution (15 µm), but this higher resolution was applied only to a few samples. A two-fold increase of the linear resolution requires 16 times longer scan times and eight times more data space. Nevertheless, if very accurate results are needed higher resolution scans should be chosen.

Last but not least, it is important to mention that µCT is not a cheap method (one scan easily cost a few hundred dollars). However, µCT is non-destructive. Moreover, the combination of the right analytical software (as shown here) with µCT data provides the fastest and cheapest method to determine the 3D macropore size distribution of a bone substitute. There are indeed other methods to characterize the porous structure of blocks but they tend to only give a partial information (e.g. permeability measurements), to be very time and costintensive (optical analysis of very thin parallel slices), or to be inapplicable for macropores (gas adsorption, Hg porosimetry).

5. Conclusion

The synthesis method based on calcium phosphate emulsions leads to reproducible and controlled structures. Indeed, the macropore size can be modified very easily with the emulsifier concentration without modifying the total pore volume and the microporosity. The pore size distribution appears to be narrow and distributed normally. Finally, the method leads to a certain number of interconnections, but the structure does not appear to be fully interconnected. More oil should probably be used to achieve a higher degree of interconnectivity.

µCT is a very good tool to characterize the micro-, macro- and total porosity of calcium phosphate ceramic blocks. Its biggest advantage over histological techniques is that is fully non-destructive and therefore the samples can be kept intact for the analysis. This allows additional testing of the samples, e.g. mechanical testing, on the same samples which improves statistics and therefore reduces sample number. Moreover, it enables a fast determination of the pore size distribution. However, limitations were observed when the macropore diameter was only a few times larger than the resolution of the µCT scan. In these cases, scans with higher resolution should be chosen.

References

[1] Klawitter JJ, Hulbert SF. Application of porous ceramics for the attachement of load bearing internal orthopedic applications. J Biomed Mater Res Symp 1971;2(1):161–229.

[2] Uchida A, Nade SM, McCartney EF, Ching W. The use of ceramics for bone replacement. A comparative study of three different porous ceramics. J Bone Joint Surg Br 1984;66(2):269–75.

[3] Eggli PS, Mueller W, Schenk RK. Porous hydroxyapatite and tricalcium phosphate cylinders with two different macropore size ranges implanted in the cancellous bone of rabbits. Clin Orthop 1988;232:127–38.

[4] Lu JX, Flautre B, Anselme K, Hardouin P, Gallur A, Descamps M, Thierry B. Role of interconnections in porous bioceramics on bone recolonization in vitro and in vivo. J Mater Sci Mater Med 1999;10:111–20.

[5] Chang B-S, Lee C-K, Hong K-S, Youn H-J, Ryu H-S, Chung S-S, Park K-W. Osteoconduction at porous hydroxyapatite with various pore configurations. Biomaterials 2000;21:1291–8.

[6] Chu T-MG, Orton DG, Hollister SJ, Feinberg SE, Halloran JW. Mechanical and in vivo performance of hydroxyapatite implants with controlled architectures. Biomaterials 2002;23:1283–93.

[7] Bohner M, Baumgart F. Theoretical model to determine the effects of geometrical factors on the resorption of calcium phosphate bone substitutes. Biomaterials 2004;25:3569–82.

[8] Bohner M. Calcium phosphate emulsions. Key Eng Mater 2001;192–195:765–8.

[9] Rüegsegger P, Koller B, Müller R. A microtomographic system for the nondestructive evaluation of bone architecture. Calcif Tiss Int 1996;58:24–9.

[10] Hildebrand T, Laib A, Müller R, Dequeker J, Rüegsegger P. Direct three-dimensional morphometric analysis of human cancellous bone: microstructural data from spine, femur, iliac crest, and calcaneous. J Bone Miner Res 1999;14(7):1167–74.

[11] Hildebrand T, Rüegsegger P. A new method for the model-independent assessment of thickness in three-dimensional images. J Microsc 1997;185:67–75.

[12] Sadler LY, Sim KG. Minimize solid-liquid mixture viscosity by optimizing particle size distribution. Chem Eng Progr 1991;87:68–71.